# A Novel Unit Cell and Analysis for Epsilon Negative Metamaterial

Thomas P. Weldon, Ryan S. Adams, and Raghu K. Mulagada
Department of Electrical and Computer Engineering
University of North Carolina at Charlotte
Charlotte, NC, USA
tpweldon@uncc.edu

***Abstract*— A novel unit cell and analysis are presented for a metamaterial with effective negative permittivity. The structure consists of two disks connected by a central post, and the analytic approach directly provides the electromagnetic field coupling to the resonant structure. By using Ampere's circuital law in the development, the electromagnetic field effects are directly coupled to the resonant behavior of the structure. In this, the theoretical approach does not depend upon plasma resonance. The proposed structure is shown to exhibit resonant behavior with negative permittivity in a frequency band near resonance. As predicted, electromagnetic field simulations show inversion of the electric field as the frequency crosses resonance.**

## I. INTRODUCTION

Materials with negative refractive index were proposed by Veselago in 1967, where he predicted that a plane wave incident on a medium with simultaneous negative values for both permittivity and permeability would be able to propagate in that medium with negative group velocity [1]. Later, Pendry *et al.* showed that a structure consisting of extremely thin wires arranged in a lattice would have a plasma frequency in the GHz range with negative effective permittivity below that frequency [2]-[3]. Smith *et al.* were able to demonstrate a complex medium with an effective negative refractive index by coupling the negative permeability of a composite medium comprised of Split Ring Resonators (SRR) with such plasma wire structures [4]. Itoh *et al.* similarly considered Composite Right/Left Handed (CRLH) transmission lines [5].

The emergence of these new metamaterials offers the potential for designing a variety of innovative electromagnetic materials with novel properties [6]. Among these, double-negative metamaterials with negative permittivity and permeability are of particular interest, since they can support electromagnetic wave propagation. Such double negative materials are often composites as described by Smith et al. [4], consisting of an arrangement of both negative permeability and negative permittivity structures. The present work considers the design of novel Epsilon Negative (ENG) metamaterials that exhibit negative permittivity.

In particular, a novel constituent unit cell, or particle, is presented that can be used to realize an ENG metamaterial. The proposed structure consists of two disks connected by a central post. In addition, a simple analytic approach is employed that directly provides the electromagnetic field coupling to the unit cell. The analysis is based on Ampere's circuital law and results in a straightforward method for coupling the electromagnetic field effects to the resonant behavior of the structure. Furthermore, the analysis does not depend upon plasma resonance, and avoids various assumptions of less direct LC circuit-based approaches that omit the coupling of the fields. Finally, the proposed negative-permittivity unit cell is shown to exhibit a resonant response similar to that of a magnetic unit cell SRR.

In the following, the structure of the proposed negative-permittivity unit cell is first described. Using Ampere's circuital law, the effective permittivity of the unit cell is derived. The predicted effective permittivity is shown to exhibit a resonance, with negative permittivity at frequencies above resonance. The analysis approach differs significantly from prior negative-permittivity structures in [4] and [7] that are based on plasma frequency of closely spaced wires. In the subsequent section, simulation results are given for an example structure using the HFSS electromagnetic simulator.

## II. ANALYSIS OF UNIT CELL

The unit cell of the proposed Electric Disk Resonator (EDR) structure is shown in Fig. 1. As is typical with most metamaterials, the dimension of the unit cell is much smaller than the free space wavelength of the target frequency of operation. The EDR consists of a metal post connecting two identical metal disks. The axes of the disks and post are parallel to the incident electric field impinging on the external faces of the two disks. This arrangement couples the electric field to the resonant structure, through the total electric flux at each of the disk faces. The metal post in Fig. 1 is connected between the centers of the disks. In the following analysis, Ampere's circuital law for the flux on the disk faces provides the link between the electromagnetic field and the resonant behavior of the EDR unit cell of Fig. 1.

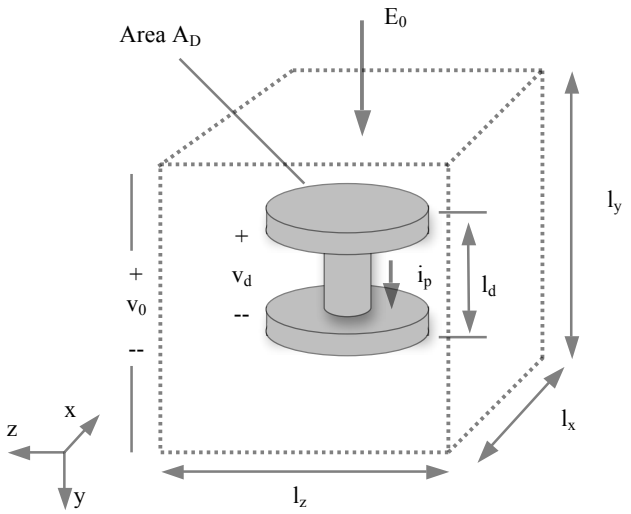


Figure 1. A unit cell of the proposed EDR structure.

For the electric disk resonator (EDR) in Fig. 1, let the dimensions of the unit cell comprising this electric metamaterial be $l_x$, $l_y$, and $l_z$ in the x, y and z directions respectively. The metal disks at the top and bottom faces of the structure have areas $A_D$, and are connected together by a metal post with inductance $L_p$. As is typical, the dimensions of the unit cell are taken to be less than 10 percent of a wavelength, so that the incident electric field intensity $E_0$ is uniform over the unit cell. Also shown in Fig. 1, the current in the post that connects the two disks is $i_p$, and the voltage between the upper and lower disk is $v_d$.

Using Ampere's circuital law, the time derivative of the electric flux at the top face of the upper disk equals the current in the post plus the time derivative of the electric flux at the bottom face of the top disk:

$$i_p + \frac{d}{dt}\Psi_F = \frac{d}{dt}\Psi_T = \frac{d}{dt}\left(\frac{\varepsilon_0 A_D v_0}{l_y - l_d}\right) = C_0\frac{dv_0}{dt}, \qquad (1)$$

where $i_p$ is the current in the post, $\Psi_T$ is the total electric flux of the top surface of the top disk of the EDR, $\Psi_F$ is the total electric flux at the bottom of the top EDR disk, the top face of the upper disk has area $A_D$, $v_o=E_0 l_y$ is the voltage across the full height of the unit cell, $C_0=\varepsilon_0 A_D/(l_y-l_d)$ is a capacitance-like parameter (effectively the capacitance between two disks of area $A_D$ and separation $l_y-l_d$), and the permittivity of free space is $\varepsilon_0=8.85\times10^{-12}$ F/m. Rearranging:

$$i_p = \frac{d}{dt}\left(v_0 C_0 - \Psi_F\right) = \frac{d}{dt}\left(v_0 C_0 - v_d C_F\right), \qquad (2)$$

where $C_F$ is the is the capacitance between the upper disk and the lower disk (acting as a leakage capacitance or fringe capacitance around the post inductance). The voltage between the two disks equals the voltage across the inductive post:

$$v_d = L_p\frac{di_p}{dt} = L_p\frac{d^2}{dt^2}\left(v_0 C_0 - v_d C_F\right), \qquad (3)$$

where $v_d$ is the voltage from the top disk to the bottom disk as before, and $L_p$ is the inductance of the metal post connecting the two disks. Taking the Laplace transform and solving for voltage gives:

$$v_d = v_0\frac{s^2 L_p C_0}{1+s^2 L_p C_F}. \qquad (4)$$

The charge on the plates gives rise to an electric dipole moment in the EDR of:

$$p = q l_d = \frac{v_d}{s^2 L_p} l_d = \frac{v_0 C_0 l_d}{1+s^2 L_p C_F}, \qquad (5)$$

where (4) was used un substituting for $v_d$ in (5), q is the charge in coulombs on the disks, p is the electric dipole moment in the same direction as $E_0$, and $l_d$ is the distance between the two disks. In (5), $q = v_d/(s^2 L_p)$, since $q=\int i_p dt$ gives $q= i_p/s$, and since $v_d = L_p di_p/dt$ gives $i_p = v_d/(sL_p)$.

Then, polarization **P** equals electric dipole moment per unit volume, so:

$$P = \frac{p}{l_x l_y l_z} = \frac{v_0 C_0 l_d}{l_x l_y l_z}\left(\frac{1}{1+s^2 L_p C_F}\right) = \frac{\varepsilon_0 E_0 l_y}{l_y - l_d}\frac{A_D l_d}{l_x l_y l_z}\left(\frac{1}{1+s^2 L_p C_F}\right), \qquad (6)$$

where $E_0 l_y = v_0$. Because $\mathbf{P} = \chi_e \varepsilon_0 \mathbf{E}$ and $\varepsilon_r = 1+\chi_e$, it follows that

$$\varepsilon_r = 1+\chi_e = 1+\frac{l_y}{l_y - l_d}\frac{\Upsilon_{EDR}}{\Upsilon_U}\left(\frac{1}{1+s^2 L_p C_F}\right), \qquad (7)$$

where $\Upsilon_{EDR} = A_D l_d$, is the volume of the EDR; $\Upsilon_U = l_x l_y l_z$, is the volume of the unit cell, $\chi_e$ is the electric susceptibility, $\omega$ is the angular frequency in rad/s, and $\varepsilon_r$ is the effective relative permittivity of the metamaterial. Commonly, this is expressed as

$$\varepsilon_r = 1+\frac{l_y}{l_y - l_d}\frac{\Upsilon_{EDR}}{\Upsilon_U}\left(\frac{\omega_{oe}^2}{\omega_{oe}^2 - \omega^2}\right), \qquad (8)$$

where $\omega_{oe} = (L_p C_F)^{-0.5}$ is the electric resonance frequency. The resulting expression in (8) forms the basis for the proposed negative-permittivity metamaterials, where $\varepsilon_r$ becomes a large negative value at frequencies where the denominator $\omega_{oe}^2 - \omega^2$ is a small negative number, indicating a reversal in the field produced by the disks.

The variation of the effective permittivity with frequency in (8) is plotted in Fig. 2 for $f_{oe} = \omega_{oe}/(2\pi) = 10$ GHz. As the frequency approaches the resonance at 10 GHz, the effective permittivity increases to a large positive value. After resonance, the effective permittivity quickly switches to a large negative value.

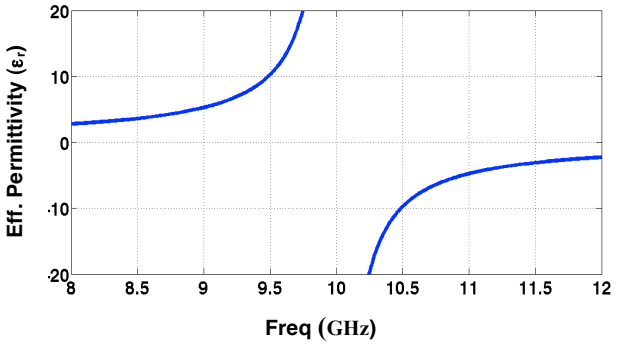


Figure 2. Effective permittivity is plotted as function of frequency with 10 GHz resonant frequency.

## III. SIMULATIONS

To verify the behavior of the EDR unit cell of Fig. 1, an example was designed for operation around 10 GHz and is shown in Fig 3. From (8), it can be seen that the effective permittivity is negative above the resonant frequency of the unit cell. The electric resonance frequency is dependent on the leakage capacitance between the plates $C_F$ and the post inductance $L_p$. The leakage capacitance $C_F$ is first estimated based on dimensions of disks in the EDR unit cell as:

$$C_F = \varepsilon_0 A_D / l_d = \varepsilon_0 \pi r_c^2 / l_d, \qquad (9)$$

where $r_c$ is the radius of disks and $l_d$ is the distance between the two disks. The inductance of the post $L_p$ can be approximated using the equation for inductance of a straight wire at high frequencies:

$$L_p = 2\times10^{-7} \cdot l_d \left( \ln\left( \frac{2l_d}{r_p} \right) - 1 \right), \qquad (10)$$

where $r_p$ is the radius of the post and $l_d$ is the length of the post, both in meters. With values of $r_c$ = 1.7 mm, $r_p$= 0.025 mm, and $l_d$ = 3 mm, the leakage capacitance given by (9) is $C_F = 2.68\times10^{-14}$ F and the post inductance given by (10) is $L_p = 2.69\times10^{-9}$ H. The estimated resonant frequency for these values is $\omega_{oe} = (C_F L_p)^{-0.5} = 1.18\times10^{11}$ rad/s or 18.7 GHz, and is likely to be a high estimate since fringing capacitances at the sharp edges of the disk are not included. For the present large aspect ration of $l_d / r_p$ = 1.76, the fringing causes the capacitance $C_F$ to approximately triple [8]. With $C_F$ tripled, the predicted resonant frequency would fall to 10.8 GHz.

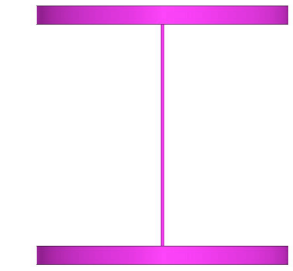

Figure 3. EDR model used in simulations consisting of top and bottom disks of radius $r_c$ = 1.7 mm connected by a post of radius $r_p$= 0.025 mm and length $l_d$ = 3 mm.

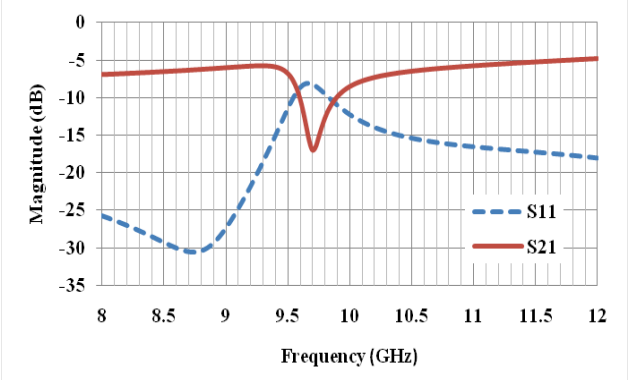


Figure 4. Simulated s-parameters of EDR unit cell showing magnitude of of $S_{11}$,(dashed blue) and $S_{21}$ (solid red).

The EDR unit cell was simulated in HFSS inside a rectangular X-band WR-90 waveguide (8-12 GHz) to characterize its resonance. Scattering parameters of the simulated EDR unit cell are shown in Fig. 4. From the magnitudes of the reflection and transmission coefficients, it can be observed that the unit cell has a resonance at 9.7 GHz, in moderate agreement with the fringe-corrected prediction of 10.8 GHz. This is slightly lower than calculated and is attributed to the difficulty in estimating the fringe capacitance accurately. Nevertheless, the error between the calculated and the observed frequencies is only 10%.

Equation (8) predicts negative permittivity above resonance, as illustrated in the example plot of Fig. 2. To observe the predicted enhancement and reversal of the electric field direction, the EDR of Fig. 3 was simulated using the HFSS electromagnetic simulation software. The incident electric field at 9.6 GHz is shown as the 1 kV/m upward green arrows in the top right of Fig. 5, just below the 9.7 GHz resonant frequency. The total electric field in the presence of the EDR is shown as the 2 kV/m upward red arrows in the bottom right of Fig. 5, and is observed to be in the same direction as the incident electric field. The observed total field is significantly stronger than the incident field, as predicted from (8) where the effective permittivity $\varepsilon_r$ is a large positive value just below the resonant frequency.

Just above the resonant frequency, the effective permittivity $\varepsilon_r$ from (8) is predicted to become a large negative value. The incident electric field at 9.8 GHz is shown as the 1 kV/m upward green arrows in the top right of Fig. 6, just above the 9.7 GHz resonant frequency. The total electric field in the presence of the EDR is shown as the 2 kV/m downward red arrows in the bottom right of Fig. 6, and is observed to be in the *opposite direction* as the incident electric field. The observed total field is significantly stronger than the incident field, as predicted from (8) where the effective permittivity $\varepsilon_r$ is a large negative value just above the resonant frequency. The reversal in the direction of the total electric field occurs over a small span of only 200 MHz, as predicted in the resonant behavior of (8).

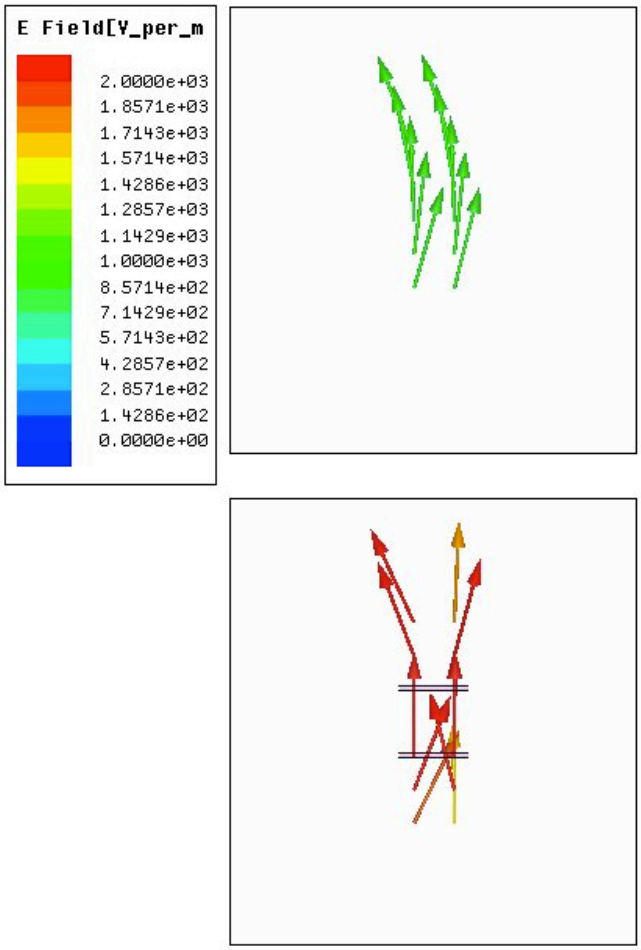


Figure 5. Electric field simulation of EDR unit cell showing the field above the top disk and below the bottom disk at 9.6 GHz, just below the 9.7 GHz resonant frequency the EDR. Upper right box shows green upward arrows indicating an incident electric field at 1 kV/m. Lower right box shows EDR with red arrows indicating an upward total field of 2 kV/m. Other surrounding fields were cropped, boundaries are radiation boundaries.

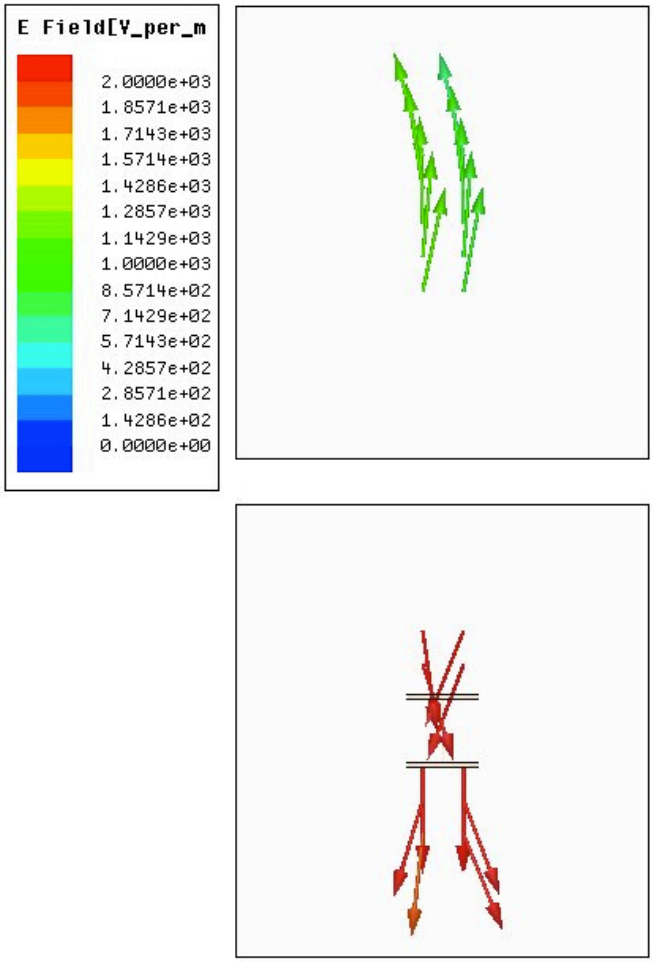


Figure 6. Electric field simulation of EDR unit cell showing the field above the top disk and below the bottom disk at 9.8 GHz, just above the 9.7 GHz resonant frequency the EDR. Upper right box shows green upward arrows indicating an incident electric field at 1 kV/m. Lower right box shows EDR with red arrows indicating a downward total field of 2 kV/m. Other surrounding fields were cropped, boundaries are radiation boundaries.

## IV. Conclusion

A novel unit cell for negative permittivity metamaterials is presented with an accompanying analysis method wherein Ampere's circuital law provides a straightforward theoretical approach for coupling the electromagnetic field effects to the resonant behavior of the structure. The simulation results are shown to be in agreement with the analytical predictions, showing resonant behavior and reversal of the electric field above resonance.

## References

[1] V. G. Veselago, "The Electrodynamics of Substances with Simultaneously negative values of ε and μ," *Soviet Physics Uspekhi **10**(4),* pp. 509, 1967.

[2] J. B. Pendry, A. J. Holden et al., "Extremely low frequency Plasmons in metallic Mesostructures," *Phys. Rev. Lett*., vol.76, no.25, pp. 4773-4776, Jun 1996.

[3] J. B. Pendry et al., "Magnetism from conductors and enhanced nonlinear phenomena," *IEEE Trans. on Microw. Theory and Tech.,* vol. 47, no.11, pp. 2075 - 2084, Nov 1999.

[4] D. R. Smith et al., "Composite medium with simultaneously negative permeability and permittivity," *Phys. Rev. Lett.,* vol. 84, no.18, pp. 4184–4187, 2000.

[5] T. Itoh et al., "Composite right/left-handed transmission line meta-materials," *IEEE Microw. Mag.,* vol. 5, no.3, pp. 34 - 50, Sep. 2004.

[6] J. B. Pendry et al., "Controlling electromagnetic fields," *Science Magazine.,* vol. 312, no.5781, pp. 1780-1782, June 2006.

[7] R. W. Ziolkowski, "Design, fabrication, and testing of double negative metamaterials," *IEEE Trans. of Antennas and Propag.,* vol. 51, no.7, pp. 1516 - 1529, July 2003.

[8] C. Y. Kim, "A numerical solution for the round disk capacitor by using annular patch subdomains," *Progress In Electromagnetics Research B*, vol. 8, pp.179-194, 2008.